Submitted to *Waves in Random and Complex Media*
Vol. 00, No. 00, Month 20XX, 1–29

Forward and backward probabilistic inference of the sea clutter

C. J. Roussel[a*], A. Coatanhay[a], A. Baussard[a]

[a]*ENSTA Bretagne, Lab-STICC (UMR CNRS 6285), 2 rue François Verny, 29806 Brest Cedex 9, France*;

(*submitted September 2017*)

The fast dynamics of the sea surface result in highly volatile time series of the sea clutter. Measures made by a moving sensor which observes the sea from different points of view cannot be compared directly if the clutter has significantly evolved during the sampling interval. The issue of transporting measures to a common time reference is addressed using a model in which the sea clutter and associated observables are homogeneous Markov processes described by stochastic differential equations. We solve the Fokker-Planck equations of the speckle and radar cross-section (RCS) to obtain their present to future transition probabilities, from which we derive those of the intensity and the real and imaginary parts of the reflectivity. Using Bayes's formula and the independence property of the speckle and RCS, we show that the formula remain valid for the present to past transition probabilities. Numerical distributions are systematically computed and match the analytical distributions. The resulting two-way prediction capability can be used to probabilistically balance the dynamics of the sea clutter. A series of deterministic measures from different positions and times is transformed into a series of probabilistic measures from different positions at the same time.

Keywords: sea clutter, stochastic differential equation, Markov processes, transition probabilities, Fokker-Planck equation

1. Introduction

In the context of radar observation of the sea surface, it is common practice to measure the signal reflected by the same area from different points of view, for example using a moving sensor (figure 1), for a time span of about $0.5 - 1$ s. It is well known that the sea clutter typically decorrelates over shorter durations [1], [2]. It makes the comparison between successive measures problematic since the sea clutter has evolved not only because of the space interval but also because of the time interval. More generally, any two measures from possibly different sensors should be made at the same time for a proper integration. As illustrated in figure 1, to every point of view corresponds a sea clutter random process with a stationary distribution (under constant weather conditions). This process can be written $X_t^{(u)}$ where t is the time parameter and u the position of the sensor. Of course, for any u_1, u_2, there is a correlation between $X_t^{(u_1)}$ and $X_t^{(u_2)}$, which starts from 1 if $u_1 = u_2$ and decreases as $|u_1 - u_2|$ increases. This dependency is not treated in this paper. We only make the hypothesis that for all u, the $X_t^{(u)}$ are described by the same

*Corresponding author. Email: clement.roussel@ensta-bretagne.org

model (Field's model, [3], see below). Our objective is to understand the time dependency only, in order to compensate it independently for each of the measures $\tilde{X}_{t_1}^{(u_1)}, \tilde{X}_{t_2}^{(u_2)} ... \tilde{X}_{t_n}^{(u_n)}$ and bring them together to a common time. Therefore, in this article we will not refer to the space parameter u. We denote simply X_t the sea clutter process from any arbitrarily chosen point of view, and $\tilde{X}_t$ its measures (or realizations).

Statistical models are generally used to describe the sea clutter (Rayleigh distribution, K distribution etc) [4]. These models provide a probability density for the sea clutter X_t that is valid for any time t (stationarity). They are static in the sense that they do not precisely model the time dependency of the sea clutter. The only clues on the relation between X_{t_1} and X_{t_2} for $t_1 \neq t_2$ are decorrelation times, which give an order of magnitude of how long it takes for the sea clutter to decorrelate. A more general and suited model for describing the time-dependency can be better.

Field's theory [3] starts from the fundamental idea that the received signal from any random media is a sum of contributions from dynamic scatterers of a random population. By taking the limit for very large populations of scatterers, Field demonstrates that the reflectivity and associated quantities (speckle, radar cross-section, intensity...) are solutions to stochastic differential equations, which are the equivalent of ordinary differential equations for random variables. The very large range of applications of this theory comprises sea clutter [5]. In this model, the sea clutter is represented as the compound of a fast Rayleigh-distributed speckle and a slow gamma-distributed texture or radar cross-section ([1], [4] for a review, [6]).

Stochastic differential equations (SDE) describe the time dependency of a random variable from any initial condition to infinite times. If the intensity is measured at some time t_0, Field's SDE expresses how the distribution of the intensity conditioned by the measure evolves from a Dirac distribution to the classical K distribution for large times, with a variance growing from 0 to a finite strictly positive limit. In Field's model, the K distribution arises as asymptotical distributions. It is therefore important to notice that Field's model encompasses the K distribution model and provides a description of the transition (or conditioned, see section 2) probabilities that the K distribution and similar models (Weibull and log-normal distributions) do not provide. Actual data validate the K distribution model and reveal that the speckle variation timescale is 10 ms while the texture (radar cross-section, denoted RCS) variation timescale is about 1 s [1], [2].

Users of radar sea-clutter may be interested in different 'observables' in accordance with their applications (Oceanography, Geophysics, maritime surveillance etc). That is why we treat systematically the speckle, RCS, intensity and real reflectivity (real part of the complex reflectivity). The imaginary part of the reflectivity is shown to have the same properties as its real part. For each of these observables, we give mathematical expressions of the transition probabilities from present to future and from present to past which enable respectively forward and backward 'probabilistic inferences'.

In section 2 precisely, we introduce vocabulary and notations to define what is meant by forward and backward probabilistic inferences, in relation with conditioned probabilities and Markov processes. We also review Field's approach and main results. In section 3, we solve the Fokker-Planck equations of the speckle and the RCS, to obtain their transition probabilities, from which we derive also the transition probabilities of the intensity and reflectivity. Numerical simulations are systematically made and give numerical distributions which match the analytical distributions. In section 4, we show that reversal of the conditioned probabilities

gives identical formula. All previous results, which were valid for forward probabilistic inferences, extend to backward probabilistic inferences. Section 5 is a discussion of the applicability of our results to address the problem of carrying measures of the sea clutter from different points of view to the same time. Section 6 concludes.

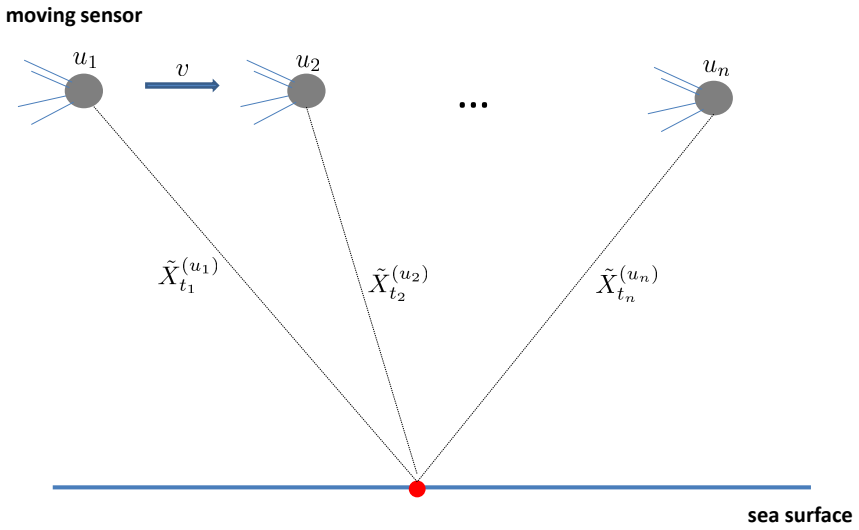

Figure 1. Moving sensor measuring the sea clutter $X_t^{(u)}$ at positions $u_1, u_2 ... u_n$ and times $t_1, t_2 ... t_n$. $\tilde{X}_t^{(u)} = X_t^{(u)}(\omega)$ is one realization of the process.

2. Theoretical background

2.1. *Forward and backward probabilistic inferences*

The foregoing section introduces the formalism and notations which will be used throughout this paper. The speckle and RCS are solutions to SDE written in section 2.2. The intensity and real and imaginary parts of the reflectivity are also solutions to SDE but we will not refer to them as explained later. A SDE is in the following form:

$$\begin{cases} \mathrm{d}X_t = \mu(X_t, t)\mathrm{d}t + \sigma(X_t, t)\mathrm{d}W_t \\ X_0 = \xi_0 \end{cases} \tag{1}$$

where $(W_t)_t$ is a brownian motion, also called Wiener process, and ξ_0 is the initial condition which can be for a time different from 0. μ is called the 'drift' and σ is called the 'volatility'. Under the conditions of Ito's theorem of existence and unicity of the solutions, the unique solution, denoted $(X_t)_{t\geq 0}$ is a Markov process (e.g. [7] p 171). We assume that it is real-valued. Let $s, t \in \mathbb{R}^+$ such that $s < t$ and $x \in \mathbb{R}$. The transition probability is the probability measure $A \mapsto p(X_t \in A | X_s = x)$ where A belongs to the Borel σ-algebra, also denoted $p(X_t \in . \, | X_s = x)$. It should be understood that $p(X_t \in A | X_s = x)$ is an intuitive notation for $\mathbb{E}[\mathbf{1}_A(X_t)|X_s =$

$x]$, which is a conditional expectation. If the volatility and drift do not depend explicitely on time, the solution is an homogeneous Markov process (e.g. [7] p 172), *i.e.* its transition probabilities depend only on the time interval length:

$$p(X_t \in . \,|X_s = x) = p(X_{t-s} \in . \,|X_0 = x).$$

It is the case of the observables we work with: speckle, RCS, intensity and real and imaginary reflectivities are homogeneous Markov processes. The transition probabilities are probabilities of a random variable conditioned by another one, and can be defined from the formalism of conditional expectations. We will refer to them sometimes as transitional and sometimes as conditioned probabilities. It is assumed, for tractability, that for any observable X_t, random vectors $(X_{t_1}, X_{t_2}...X_{t_n})$ extracted from the process are absolutely continuous. The same assumption is made if extracted vectors mix up different observables. Defining conditioned probabilities in the most general case is not trivial and care should be taken when dealing with them. However, their calculus rules are quite gentle in the end. In particular, $p(X_t \in . \,|X_s = x)$ is absolutely continuous with a distribution denoted $y \mapsto p(X_t = y|X_s = x)$.

A very important result is used in sections 3 and 4: transformations and conditioning are commutative. More specifically, let X denote a $\mathbb{R}^n$ valued random vector and G a C^1-diffeomorphism between appropriate subsets of $\mathbb{R}^n$. Let Y denote a $\mathbb{R}^m$-valued random vector and $y \in \mathbb{R}^m$. We are again in the framework of absolute continuity. From what was said above, we can consider a random vector denoted $cond(X)$ with the distribution $p(cond(X) = x) = p(X = x|Y = y)$. Commutativity of conditioning and transformations is expressed by the relation:

$$p(G(X) = x|Y = y) = p(G(cond(X)) = x). \tag{2}$$

This result is used in sections 3 and 4 to compute the conditioned probability of products of independent random variables, which is a special case where we take $G : (x, y) \mapsto (xy, x)$ and then integrate to obtain the conditioned probability of the first component.

Besides the mathematical complications, $p(X_t = y|X_s = x)$ can simply be thought of as the 'probability' that X_t is equal to y knowing that X_s is equal to x (with some abuse of terminology). Knowing $p(X_t = y|X_s = x)$ enables what we refer to as a probabilistic inference, *i.e.* a statement of the form "given its value at time s, the sea clutter has a probability p to be in the interval $[a, b]$ at time t". From the deterministic measure $X_s = x$, we can infer the distribution of the possible values for X_t. Since $s < t$, it is a **forward probabilistic inference**. Using Bayes's formula, we can return the conditioned probability to obtain the **backward probabilistic inference** $p(X_s = x|X_t = y)$ (see section 4).

For any observable, $(X_t)_{t\geq 0}$ is the unique physical stochastic process observed from a fixed position. It varies with the position of the sensor but this dependency is not treated here. $\forall t \geq 0$, X_t has the stationary distribution $x \mapsto p(X_\infty = x)$, *i.e.* $p(X_t = x) = p(X_\infty = x)$. $(X_t)_t$ is solution to (1) with the initial condition ξ_0 such that $p(\xi_0 = x) = p(X_\infty = x)$. For example, Field's model gives a K distribution for the stationary distribution of the intensity, in accordance with the literature (see intro). Using the symbol '∞' makes sense from the results in section 6.1 of [8]: if the drift and volatility are not explicit functions of time, $p(X_t = x)$ tend toward the stationary solution as $t \to +\infty$ whatever the initial condition ξ_0. The stationary solution is therefore also the asymptotic one. The SDE provides a 'structure' to the process, X_s and X_t being more and more correlated as $t - s \to 0$ and less and

less correlated as $t-s \to +\infty$. This structure reveals itself when we condition the process X_t by the measure $X_s = x$. Indeed, an important property bridges a gap. Let $(X_t^{x,s})_{t\geq 0}$ be the solution to (1) with initial condition $X_s = x$, which has the Dirac distribution δ_x. It is shown in [7] p 171 that $p(X_t^{x,s} = y) = p(X_t = y|X_s = x)$. This is implictly used later when we get $p(X_t = y|X_s = x)$ from solving the SDE with a deterministic initial condition (speckle and RCS). This property also means that mathematically, conditioning the process X_t by $X_0 = x$ leads not only to conditioned probabilities, but to a brand new random process. That is why we emphasized that their is only one physical process by point of view. The processes obtained by conditioning only relates to our knowledge. We will not refer to them from now on, since writing conditional probabilities is sufficient.

2.2. *Field's model*

Field's model represents the complex-valued time-dependent electromagnetic field reflected by the sea surface as a sum of contributions from the individual scatterers of a random population. The resulting signal follows a random walk model in the complex plane [9], [10], [11]:

$$\mathcal{E}_t^{(N)} = \sum_{n=1}^{N} a e^{i\phi_t^{(n)}}. \tag{3}$$

N is the total number of scatterers, and $\phi_t^{(n)}$ is the phase of the n-th scatterer, which depends on its random position. For simplicity, the amplitude is assumed constant and equal for all scatterers. The phases are stochastic processes $\phi_t^{(n)}$ solutions to the SDE (equation (6.17) p 43 of [3]):

$$\phi_t^{(n)} = \Delta^{(n)} + \mathcal{B}^{\frac{1}{2}} W_t^{(n)}, \tag{4}$$

where $\Delta^{(n)}$ is uniformly distributed on $[0, 2\pi[$ and $W_t^{(n)}$ are independent brownian processes. $\mathcal{B}$ is a constant of the model and is homogeneous to a frequency. It represents the inverse of a decorrelation time for the phase. For all n, we have the SDE:

$$\begin{cases} \mathrm{d}\phi_t^{(n)} = \mathcal{B}^{\frac{1}{2}} \mathrm{d}W_t^{(n)} \\ \phi_0^{(n)} = \Delta^{(n)} \end{cases} \tag{5}$$

The squared-modulus $z_t^{(N)}$ of the complex-valued process $\mathcal{E}_t^{(N)}$ is a random variable with values in $\mathbb{R}^+$:

$$z_t^{(N)} = |\mathcal{E}_t^{(N)}|^2 = \langle \sum_{j=1}^{N} a e^{i\phi_t^{(j)}}, \sum_{k=1}^{N} a e^{-i\phi_t^{(k)}} \rangle = a^2 \sum_{j=1}^{N} \sum_{k=1}^{N} e^{i(\phi_t^{(j)} - \phi_t^{(k)})}.$$

The mean squared-modulus $\mathbb{E}[z_t^{(N)}]$ is proportional to the total number of scatterers. Indeed:

$$\mathbb{E}[z_t^{(N)}] = a^2 \sum_{j=1}^{N} \sum_{k=1}^{N} \mathbb{E}[e^{i(\phi_t^{(j)} - \phi_t^{(k)})}].$$

It is trivial to demonstrate that $\forall j = k$, $\mathbb{E}[e^{i(\phi_t^{(j)} - \phi_t^{(k)})}] = 1$. For $j \neq k$, we write:

$$\mathbb{E}[e^{i(\phi_t^{(j)} - \phi_t^{(k)})}] = \mathbb{E}[e^{i\phi_t^{(j)}} e^{-i\phi_t^{(k)}}] = Cov(e^{i\phi_t^{(j)}}, e^{i\phi_t^{(k)}}) = 0,$$

since $e^{i\phi_t^{(j)}}$ and $e^{i\phi_t^{(k)}}$ are independent ([3] p 43) and $\mathbb{E}[e^{i\phi_t^{(j)}}] = 0$, $\forall j$, $\forall t$. Finally, we get:

$$\mathbb{E}[z_t^{(N)}] = Na^2.$$

In Field's model, $N = N_t$ is a stochastic process. It results from a Birth-Death-Immigration model, in which scatterers can either appear (birth and immigration) or disappear (death). We denote $\bar{N}$ the time-independent expectation of N_t. We set $a = 1/\bar{N}^{\frac{1}{2}}$ to ensure a constant expectation of the squared-modulus as we raise $\bar{N}$ (or partition a portion of the sea surface in more weaker contributing subpieces). We get:

$$\mathcal{E}_t^{(N_t)} = \frac{1}{\bar{N}^{\frac{1}{2}}} \sum_{n=1}^{N_t} e^{i\phi_t^{(n)}} = \left(\frac{N_t}{\bar{N}}\right)^{\frac{1}{2}} \frac{1}{N_t^{\frac{1}{2}}} \sum_{n=1}^{N_t} e^{i\phi_t^{(n)}}.$$

The complex-valued reflectivity, Ψ, is defined by the following limit (equation 8.3 p 53 of [3]):

$$\Psi_t = \lim_{\bar{N}\to+\infty} \mathcal{E}_t^{(N_t)} = \lim_{\bar{N}\to+\infty} \left(\frac{N_t}{\bar{N}}\right)^{\frac{1}{2}} \lim_{\bar{N}\to+\infty} \frac{1}{N_t^{\frac{1}{2}}} \sum_{n=1}^{N_t} e^{i\phi_t^{(n)}},$$

which can be written :

$$\Psi_t = x_t^{\frac{1}{2}}\, \gamma_t, \tag{6}$$

with $x_t = \lim_{\bar{N}\to+\infty} \left(\frac{N_t}{\bar{N}}\right)$ and $\gamma_t = \lim_{\bar{N}\to+\infty} \frac{1}{N_t^{\frac{1}{2}}} \sum_{n=1}^{N_t} e^{i\phi_t^{(n)}}$. γ_t is the fast varying speckle and x_t the slow varying texture in [1], [2]. x_t is what we call the RCS in this context. It is the limit of the ratio between the actual number of scatterers and the mean number of scatterers. By construction, $\mathbb{E}[x_t] = 1$. γ_t is a complex valued process which we write

$$\gamma_t = \gamma_t^{(R)} + i\gamma_t^{(I)}, \tag{7}$$

where 'i' denotes the imaginary unit. Thus, the complex reflectivity can be written:

$$\Psi_t = x_t^{1/2} \left(\gamma_t^{(R)} + i\gamma_t^{(I)}\right) = x_t^{1/2}\gamma_t^{(R)} + ix_t^{1/2}\gamma_t^{(I)} = I_t + iQ_t. \tag{8}$$

I_t, Q_t are respectively the real (in-phase) and imaginary (quadrature phase) components of the complex reflectivity Ψ_t.

The intensity is defined as the squared-modulus of Ψ_t. It is denoted z_t and we have:

$$z_t = |\Psi_t|^2 = x_t \left(\gamma_t^{(R)\,2} + \gamma_t^{(I)\,2}\right). \tag{9}$$

Finally, let θ_t be the phase of Ψ_t in $]-\pi,\pi]$. We write:

$$\theta_t = \theta(\Psi_t) = \theta(\gamma_t). \tag{10}$$

We remind that θ_t is not treated below in section 3 and 4. The complex-valued reflectivity can therefore also be written:

$$\Psi_t = \sqrt{z_t} e^{i\theta_t}. \tag{11}$$

Note that the speckle γ_t does not necessarily have a unit modulus. However, $\mathbb{E}[|\gamma_t|^2] = 1$. From $\mathbb{E}[z_t^{(N)}|N_t = N] = N/\bar{N}$, we can show that $\mathbb{E}[z_t|x_t = x] = x$, which means that a constant RCS is simply the expectation of the intensity process. It is consistent with the K distribution model [4].

We have defined all the observables we treat in this paper or may refer to: $\Psi_t, \gamma_t^{(R)}$, $\gamma_t^{(I)}$, x_t, I_t, Q_t, z_t, θ_t. We see from equations (8) and (9) that it is sufficient to have $x_t, \gamma_t^{(R)}, \gamma_t^{(I)}$ to compute the other observables. We choose to write 2 real-valued equations for $\gamma_t^{(R)}, \gamma_t^{(I)}$ respectively instead of one complex-valued equation for γ_t as in [3] p 53. The SDE for a scaled version of the RCS is given p 54 in [3] but we express it here for the original RCS as defined previously. We obtain the 3 SDE:

$$\begin{cases} \mathrm{d}(x_t) = \mathcal{A}(1-x_t)\mathrm{d}t + \left(2\frac{\mathcal{A}}{\alpha}x_t\right)^{\frac{1}{2}} \mathrm{d}W_t^{(x)} \\ \mathrm{d}\gamma_t^{(R)} = -\frac{1}{2}\mathcal{B}\gamma_t^{(R)}\mathrm{d}t + \frac{1}{\sqrt{2}}\mathcal{B}^{\frac{1}{2}}\mathrm{d}W_t^{(R)} \\ \mathrm{d}\gamma_t^{(I)} = -\frac{1}{2}\mathcal{B}\gamma_t^{(I)}\mathrm{d}t + \frac{1}{\sqrt{2}}\mathcal{B}^{\frac{1}{2}}\mathrm{d}W_t^{(I)} \end{cases} \tag{12}$$

where $W_t^{(x)}, W_t^{(R)}, W_t^{(I)}$ are 3 independent brownian motions. 3 constants parameterize the model: $\mathcal{A}$ and α for the RCS, and $\mathcal{B}$ for $\gamma_t^{(R)}$ and $\gamma_t^{(I)}$. $\mathcal{A}$ and α are from the underlying Birth-Death-Immigration population model for the number of scatterers.

It is noteworthy that in [3] the SDE for the RCS was first expressed as:

$$\mathrm{d}x_t = \nu(1-x_t)\mathrm{d}t + (2\lambda x_t)^{\frac{1}{2}}\mathrm{d}W_t^{(x)}, \tag{13}$$

where λ, μ, ν are respectively the birth, death and immigration rates of the scatterers population (see [3] chapter 7). Setting $\mu = \lambda$, $\mathcal{A} = \nu$ and $\alpha = \frac{\nu}{\lambda}$ yields the first equation of (12).

$\mathcal{A}$ and $\mathcal{B}$ are homogeneous to the inverse of a time (*i.e.* a frequency). $\mathcal{A}$ can be understood as the inverse of a decorrelation time for the RCS, and $\mathcal{B}$ as the inverse of a decorrelation time for the speckle. It will be more visible from the analytical expressions of the transition probabilities of the speckle and RCS in section 3. We already mentionned that the order of magnitude of the decorrelation times are 1 s for the RCS and 10 ms for the speckle. Therefore, we set $\mathcal{A} = 1$ Hz and $\mathcal{B} = 100$ Hz in the following.

To first order, γ_t and x_t are independent since x_t is related to the number of scatterers while γ_t is related to their spatial disposition. We also assume that $\gamma_t^{(R)}$ and $\gamma_t^{(I)}$ are independent. To support that hypothesis, we note that they are solutions to SDE whose brownian processes are independent.

3. Present to future transition probabilities

Present to future transition probabilities are of the form $p(X_t = x|X_s = y)$ where $s \leq t$. Analytical expressions can be obtained solving the Fokker Planck (a.k.a Kolmogorov forward) equations. In what follows when solving the Fokker Planck equations (FPE), 'p' refers to $p(X_t = x|X_0 = y)$ in the time-dependant case, and to $p(X_\infty = x) = p(X_t = x)$ in the stationary case. We remind that by homogeneity, $p(X_t = x|X_s = y) = p(X_{t-s} = x|X_0 = y)$. In this section, the FPE are expressed and solved for the speckle γ_t and the RCS x_t only. Afterwards, the transition probabilities of the intensity and real (and imaginary) reflectivity are obtained using the relations (8), (9) and the rules of calculus for conditioned probabilities (see section 2.1).

3.1. *Distributions of the speckle*

$\gamma_t^{(R)}$ and $\gamma_t^{(I)}$ are real-valued Ornstein-Ulhenbeck processes (e.g. [12]). They are solution to the same SDE given in (12), only the driving brownian motion changes. It is therefore sufficient to study $\gamma_t^{(R)}$ for example. From its SDE, we can write its FPE (see appendix A.3):

$$\frac{\partial p}{\partial t} = \frac{\mathcal{B}}{4}\frac{\partial^2 p}{\partial^2 x} + \frac{1}{2}\mathcal{B}\frac{\partial x\, p}{\partial x}. \tag{14}$$

3.1.1. Stationary probability

The stationary FPE for $\gamma_t^{(R)}$ reads:

$$0 = \frac{\mathcal{B}}{4}\frac{\partial^2 p}{\partial^2 x} + \frac{1}{2}\mathcal{B}\frac{\partial x\, p}{\partial x}, \tag{15}$$

which can also be written ([8] section 5.2):

$$\begin{aligned} &-\left(-\tfrac{1}{2}\mathcal{B}x\right)p + \frac{\partial}{\partial x}\left(\frac{\mathcal{B}}{4}p\right) = 0 \\ \Leftrightarrow\ &\frac{-\frac{1}{2}\mathcal{B}x}{\mathcal{B}/4}\frac{\mathcal{B}}{4}p = \frac{\partial}{\partial x}\left(\frac{\mathcal{B}}{4}p\right), \end{aligned}$$

the solution of which reads [8]:

$$\begin{aligned} p(x) &= \frac{C}{\mathcal{B}/4}\, exp\left(\int_0^x \frac{-\frac{1}{2}\mathcal{B}u}{\mathcal{B}/4}du\right) \\ \Leftrightarrow p(x) &= \frac{C}{\mathcal{B}/4}\, e^{-x^2}. \end{aligned}$$

where $C \in \mathbb{R}$ is a constant. Using $\int_{\mathbb{R}} p(x)dx = 1$, this constant is given by $C = \frac{\mathcal{B}}{4\sqrt{\pi}}$. Finally, the stationary distribution is:

$$p\left(\gamma_\infty^{(R)} = x\right) = p\left(\gamma_\infty^{(I)} = x\right) = \frac{1}{\sqrt{\pi}}e^{-x^2}. \tag{16}$$

It is a centered gaussian random variable of variance 1/2. Since the unconditioned physical speckle is stationary, we have for all $t \geq 0$:

$$p\left(\gamma_t^{(R)} = x\right) = p\left(\gamma_t^{(I)} = x\right) = p\left(\gamma_\infty^{(R)} = x\right).$$

3.1.2. Transition probabilities

$\gamma_0^{(R)}$ is the real-part of the speckle at time $t = 0$, whose distribution is given by equation (16). Let $y \in \mathbb{R}$ and let assume that we measured $\tilde{\gamma}_0^{(R)} = y$. Taking this present measure into account to predict how the speckle is going to evolve in the future is equivalent to computing the conditioned probability $p\left(\gamma_t^{(R)} = x | \gamma_0^{(R)} = y\right)$, which is solution to the FPE (14) with the initial distribution $p(x) = \delta_y(x)$. The Fokker-Planck equation for an Ornstein-Ulhenbeck process is solved p 100 of [8] using the Fourier transform. $\forall x \in \mathbb{R}$, $\forall t > 0$, the solution is given by a gaussian distribution:

$$p\left(\gamma_t^{(R)} = x | \gamma_0^{(R)} = y\right) = \frac{1}{\sqrt{2\pi v(t)}} e^{-\frac{1}{2}\frac{(x-m(t))^2}{v(t)}}, \tag{17}$$

with expectation:

$$m(t) = y e^{-\mathcal{B}t/2}, \tag{18}$$

and variance:

$$v(t) = \frac{1 - e^{-\mathcal{B}t}}{2}. \tag{19}$$

The expectation starts from y at $t = 0$ and exponentially decays towards 0 as $t \to +\infty$. The variance starts from 0 at $t = 0$ (Dirac distribution) and increases toward $\frac{1}{2}$ as $t \to +\infty$. Therefore, there is a progressive increase in the uncertainty which nonetheless remains finite as we draw away from the initial condition.

We use the Euler-Maruyama method for solving numerically the SDE for $\gamma_t^{(R)}$ as described in appendix A.2. Normalized time-dependent histograms are computed from 10000 simulated trajectories. The results depicted in figure 2 show a very good agreement between the observed numerical histograms and the analytical distributions given by equation (17). We observe the predicted behaviour: exponential decay of the mean of the trajectories toward 0 and progressive increase of their variance toward $\frac{1}{2}$. We can better understand the link between conditioned probabilities and forward probabilistic inferences. For $t = 0.001$ s for example, the distribution is almost centered at the measure $y = 2$ and has a much smaller variance than the asymptotic distribution. We have more constraints on what the measure of $\gamma_{0.001}^{(R)}$ is likely to give than if no measure is taken into account, in which case the asymptotic distribution is the best guess.

3.2. *Distributions of the RCS*

Following Field in [3], we set $\check{x}_t = \alpha x_t$. This transformation usually results in simpler equations and more tractability. We obtain the following SDE:

$$\mathrm{d}(\check{x}_t) = \mathcal{A}(\alpha - \check{x}_t)\mathrm{d}t + (2\mathcal{A}\check{x}_t)^{\frac{1}{2}}\mathrm{d}W_t^{(x)}. \tag{20}$$

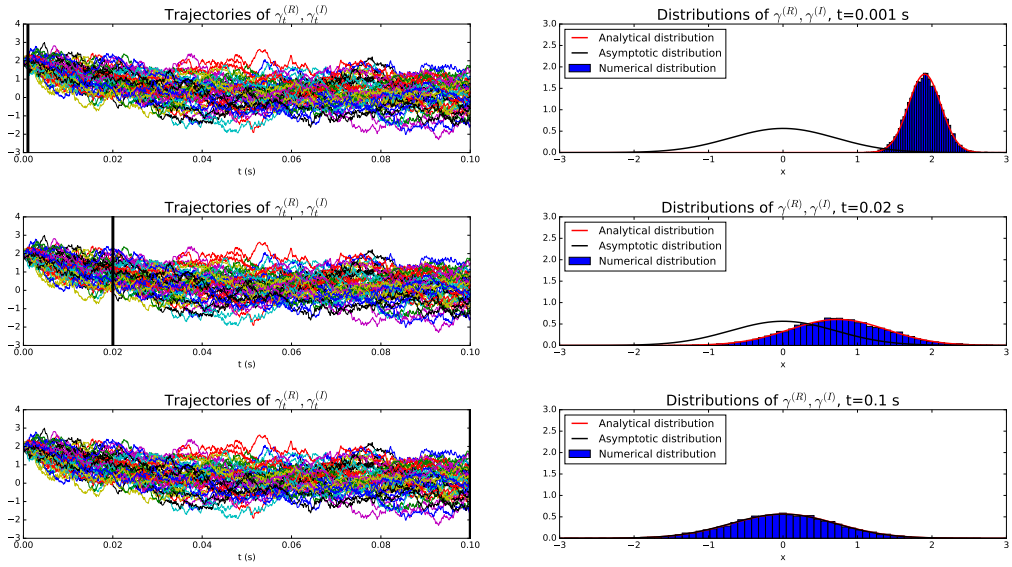

Figure 2. Comparison between analytical distributions of $\gamma_t^{(R)}, \gamma_t^{(I)}$ derived from the resolution of the FPE (equation 17), and numerical distributions from the resolutions of the SDE using the Euler-Maruyama method. 10000 trajectories are computed with $\mathcal{B} = 100$ Hz and $y = 2$.

The FPE reads (see appendix A.3):

$$\begin{aligned} \frac{\partial p}{\partial t} &= \frac{1}{2}\frac{\partial^2 2\mathcal{A}xp}{\partial^2 x} - \frac{\partial \mathcal{A}(\alpha - x)p}{\partial x} \\ \Leftrightarrow \frac{\partial p}{\partial t} &= \mathcal{A}x\frac{\partial^2 p}{\partial x^2} + \mathcal{A}(2 - \alpha + x)\frac{\partial p}{\partial x} + \mathcal{A}p \end{aligned} \tag{21}$$

From now on we assume $\mathcal{A} \neq 0$. If $\mathcal{A} = 0$, the distribution remains identical to the initial condition. If the latter is deterministic (*i.e.* $p(x, 0) = \delta_{x_0}(x)$), we have $\forall t \geq 0, p(x, t) = \delta_{x_0}(x)$, which means that the RCS remains constant and equal to x_0.

3.2.1. Stationary probability

The stationary (asymptotic) distribution is solution to:

$$0 = \mathcal{A}x\frac{\partial^2 p}{\partial x^2} + \mathcal{A}(2 - \alpha + x)\frac{\partial p}{\partial x} + \mathcal{A}p$$

It is given p 49 of [3] by:

$$p(\check{x}_\infty = x) = \frac{x^{\alpha-1}e^{-x}}{\Gamma(\alpha)}\mathbf{1}_{[0,+\infty[}(x), \tag{22}$$

where Γ denotes the usual gamma function, and $\mathbf{1}$ the indicator function. Proceeding to the inverse transform $x_t \to \check{x}_t/\alpha$, we get:

$$p(x_\infty = x) = \frac{\alpha(\alpha x)^{\alpha-1}\, e^{-\alpha x}}{\Gamma(\alpha)} \mathbf{1}_{[0,+\infty[}(x). \tag{23}$$

3.2.2. Transition probabilities

x_0 is the RCS at time $t = 0$, whose distribution is given by equation (23). Let $y \in \mathbb{R}^+$ and let assume that we measured $\tilde{x}_0 = y$. Taking this present measure into account to predict how the RCS is going to evolve in the future is equivalent to computing the conditioned probability $p\left(x_t = x | x_0 = y\right)$. It is obtained by applying the inverse transform $x_t \to \check{x}_t/\alpha$ to the solution of the FPE (21) with a Dirac initial distribution $\delta_{\alpha y}$. A direct resolution of the FPE (21) is provided in what follows. We use the asymptotic distribution (22) to gain insight into the solution we are looking for, and make the following transformation: $p(x,t) = x^{\alpha-1}\tilde{p}(x,t)$. We get:

$$\frac{\partial \tilde{p}}{\partial t} = \mathcal{A}x\frac{\partial^2 \tilde{p}}{\partial x^2} + \mathcal{A}(\alpha + x)\frac{\partial \tilde{p}}{\partial x} + \mathcal{A}\alpha\tilde{p}.$$

To obtain the solution of the FPE, we use the separation of variables $\tilde{p}(x,t) = X(x)T(t)$. The 'prime' symbol refers to derivation with respect to t when it comes after 'T' and with respect to x when it comes after 'X'. We get:

$$\begin{aligned} T'(t)X(x) &= \mathcal{A}xT(t)X''(x) + \mathcal{A}(\alpha + x)T(t)X'(x) + \mathcal{A}\alpha T(t)X(x) \\ \Leftrightarrow \frac{T'(t)}{T(t)} &= \frac{\mathcal{A}xX''(x) + \mathcal{A}(\alpha + x)X'(x) + \mathcal{A}\alpha X(x)}{X(x)} \end{aligned}$$

Thus $\exists \lambda > 0$ such that:

$$\begin{cases} T'(t) = -\lambda T(t) \\ \mathcal{A}xX''(x) + \mathcal{A}(\alpha + x)X'(x) + \mathcal{A}\alpha X(x) = -\lambda X(x) \end{cases}$$
$$\Leftrightarrow$$
$$\begin{cases} T(t) = c_\lambda e^{-\lambda t} \\ xX''(x) + (\alpha + x)X'(x) + (\alpha + \frac{\lambda}{\mathcal{A}})X(x) = 0 \end{cases} \tag{24}$$

where $c_\lambda \in \mathbb{R}^+$. We get inspiration from the exponential decay of the asymptotic distribution as $x \to +\infty$ and make the transformation $X(x) = z(x)e^{-x}$. Replacement into the second equation of (24) gives:

$$xz''(x) + (\alpha - x)z'(x) + \frac{\lambda}{\mathcal{A}}z(x) = 0,$$

which can be written:

$$xz''(x) + (b + 1 - x)z'(x) + az(x) = 0, \tag{25}$$

with $b = \alpha - 1$ and $a = \frac{\lambda}{\mathcal{A}}$. Equation (25) can equivalently be seen as a Laguerre differential equation or a confluent hypergeometric differential equation.

Its two independent solutions are (p 1481 [13]) the generalized Laguerre function $L_a^b(x) = \frac{\Gamma(a+b+1)}{\Gamma(a+1)\Gamma(b+1)}\ {}_1F_1(-a, b+1, x)$ and the confluent hypergeometric function of the second kind $U(-a, b+1, x)$ (a.k.a Tricomi's function). For $n_1, n_2 \in \mathbb{N}$, ${}_{n_1}F_{n_2}$ refers to the hypergeometric function. For more about these functions, refer to [14]. Therefore, the general solution is:

$$X(x) = d_1 L_{\frac{\lambda}{\mathcal{A}}}^{\alpha-1}(x)e^{-x} + d_2 U\left(-\frac{\lambda}{\mathcal{A}}, \alpha, x\right)e^{-x}, \tag{26}$$

with d_1, $d_2 \in \mathbb{R}$.

There is an interesting application of the generalized Laguerre functions at section 13.2 of [15]. The resolution of Schrödinger's equation for the hydrogen atom in spherical coordinates using separation of variables gives a Laguerre differential equation for the radial part. It is not explicit in this reference but the confluent hypergeometric function of the second kind is discarded because $U(a, b, 0) = \infty$ if $Re(b) > 1$ [14], which is unacceptable in their context. In our problem, we cannot discard it since $p(x_\infty = 0) = +\infty$ for $\alpha \leq 1$. Again from the asymptotic distribution, we impose an exponential decay for $x \to +\infty$ which leads to a discretization of the possible values of λ.

From [14], $U(-\frac{\lambda}{\mathcal{A}}, \alpha, x) \sim x^{\frac{\lambda}{\mathcal{A}}}$ for $x \to +\infty$, so $d_2 U(-\frac{\lambda}{\mathcal{A}}, \alpha, x)e^{-x} \sim d_2 e^{-x} x^{\frac{\lambda}{\mathcal{A}}}$ for $x \to +\infty$, which means that $\forall\lambda$, it decays exponentially. However, ${}_1F_1(-\frac{\lambda}{\mathcal{A}}, \alpha, x) \sim e^x x^{-\frac{\lambda}{\mathcal{A}}-\alpha}$ for $x \to +\infty$ if $\frac{\lambda}{\mathcal{A}} \notin \mathbb{N}$, in which case:

$$d_1 L_{\frac{\lambda}{\mathcal{A}}}^{\alpha-1}(x)e^{-x} \sim d_1 \frac{\Gamma(\frac{\lambda}{\mathcal{A}} + \alpha)}{\Gamma(\frac{\lambda}{\mathcal{A}} + 1)\Gamma(\alpha)} x^{-\frac{\lambda}{\mathcal{A}}-\alpha}.$$

The decrease is only polynomial for $x \to +\infty$. If $\frac{\lambda}{\mathcal{A}} \in \mathbb{N}$, ${}_1F_1(-\frac{\lambda}{\mathcal{A}}, \alpha-1, x)$ is a polynomial and $L_{\frac{\lambda}{\mathcal{A}}}^{\alpha-1}$ reduces to the Laguerre polynomial. In that case, $d_1 L_{\frac{\lambda}{\mathcal{A}}}^{\alpha-1}(x)e^{-x}$ decays exponentially for $x \to +\infty$. Under the constraint of exponential decay, we have narrowed down the range of possible λ to:

$$\lambda \in \{0, \mathcal{A}, 2\mathcal{A}, 3\mathcal{A}...\} = \mathcal{A}\mathbb{N}.$$

It turns out that for $\lambda \in \mathcal{A}\mathbb{N}$, *i.e.* for $-\frac{\lambda}{\mathcal{A}} \in -\mathbb{N}$, we get [14]:

$$U\left(-\frac{\lambda}{\mathcal{A}}, \alpha, x\right) = U(-n, \alpha, x) = (-1)^n n! L_n^{\alpha-1}(x).$$

The general solution of (24) reduces to $X(x) = dL_{\frac{\lambda}{\mathcal{A}}}^{\alpha-1}(x)e^{-x}$, where $d \in \mathbb{R}$. The general solution of (21) reads:

$$p(x,t) = \sum_{n=0}^{+\infty} c_n e^{-\mathcal{A}nt} e^{-x} x^{\alpha-1} L_n^{\alpha-1}(x). \tag{27}$$

It is well known that $\{L_n^{\alpha-1},\ n \in \mathbb{N}\}$ is a family of orthogonal polynomial [16]. If

$\alpha - 1 > -1$, $\forall n, m \in \mathbb{N}$:

$$\langle L_n^{\alpha-1}, L_m^{\alpha-1} \rangle_{e^{-x}x^{\alpha-1}} = \int_0^{+\infty} L_n^{\alpha-1}(x) L_m^{\alpha-1}(x) e^{-x} x^{\alpha-1} dx = \frac{\Gamma(n+\alpha)}{n!} \delta_{n,m}. \quad (28)$$

Using (28), we compute the c_n coefficients:

$$\begin{aligned}
\langle p(.,t), L_k^{\alpha-1} \rangle &= \int_0^{+\infty} \sum_{n=0}^{+\infty} c_n e^{-\mathcal{A}nt} e^{-x} x^{\alpha-1} L_n^{\alpha-1}(x) L_k^{\alpha-1}(x) dx \\
&= \sum_{n=0}^{+\infty} \int_0^{+\infty} c_n e^{-\mathcal{A}nt} e^{-x} x^{\alpha-1} L_n^{\alpha-1}(x) L_k^{\alpha-1}(x) dx \\
&= c_k e^{-\mathcal{A}kt} \frac{\Gamma(k+\alpha)}{n!} \\
\Leftrightarrow c_n &= \langle p(.,t), L_n^{\alpha-1} \rangle e^{-\mathcal{A}nt} \frac{n!}{\Gamma(n+\alpha)}
\end{aligned}$$

At $t = 0$ and with the Dirac initial condition $p(x, 0) = \delta_{\alpha y}(x)$, the c_n coefficients reduce to:

$$\begin{aligned}
c_n &= \langle \delta_{\alpha y}, L_n^{\alpha-1} \rangle \frac{n!}{\Gamma(n+\alpha)} \\
&= L_n^{\alpha-1}(\alpha y) \frac{n!}{\Gamma(n+\alpha)}. \quad (29)
\end{aligned}$$

Replacing the c_n coefficients in (27) by their expression (29), we obtain that $\forall x \in \mathbb{R}$ and $\forall t > 0$:

$$p(\check{x}_t = x | \check{x}_t = \alpha y) = \sum_{n=0}^{+\infty} \frac{L_n^{\alpha-1}(\alpha y) n!}{\Gamma(n+\alpha)} e^{-\mathcal{A}nt} e^{-x} x^{\alpha-1} L_n^{\alpha-1}(x) \mathbf{1}_{[0,+\infty[}(x).$$

This is equation 8.55 of [3], which was given without an explicit proof. Applying the inverse transform $x_t \to \frac{\check{x}_t}{\alpha}$, we finally obtain the transient distributions of the RCS x_t:

$$p(x_t = x | x_0 = y) = \sum_{n=0}^{+\infty} \frac{\alpha L_n^{\alpha-1}(\alpha y) n!}{\Gamma(n+\alpha)} e^{-\mathcal{A}nt} e^{-\alpha x} (\alpha x)^{\alpha-1} L_n^{\alpha-1}(\alpha x) \mathbf{1}_{[0,+\infty[}(x). \quad (30)$$

We use the Milstein method for solving numerically the SDE for x_t as the Euler-Maruyama method revealed itself insufficient: it generated negative values, which is impossible for the RCS, and ended the computation. Normalized time-dependent histograms are computed from 10000 simulated trajectories. The results depicted in figure 3 show that there is an accurate agreement between the numerical and analytical distributions. However, oscillations appears in the analytical solution for t close to 0, which can be due to the fact that we we were able to compute the sum in (30) up to $n = 150$ only. That is the approximate limit of Python for computing $n!$ and $\Gamma(n + \alpha)$. To go beyond, one could compute and approximate of the ratio $\frac{n!}{\Gamma(n+\alpha)}$ which should evolve much more slowly than $n!$ and $\Gamma(n +$

α) since $n! = \Gamma(n+1)$. Another issue is the computing time for evaluating the Laguerre polynomials for large n. We observe the progressive variance increase of the conditioned distributions, as well as their convergence toward the asymptotic distribution as $t \to +\infty$. It illustrates again the difference between $p(x_t = x|x_0 = y)$ and $p(x_t = x)$, which is asymptotically distributed. There is a gain in using the distribution $p(x_t = x|x_0 = y)$ rather than $p(x_t = x)$ to infer the future measure $\tilde{x}_t$.

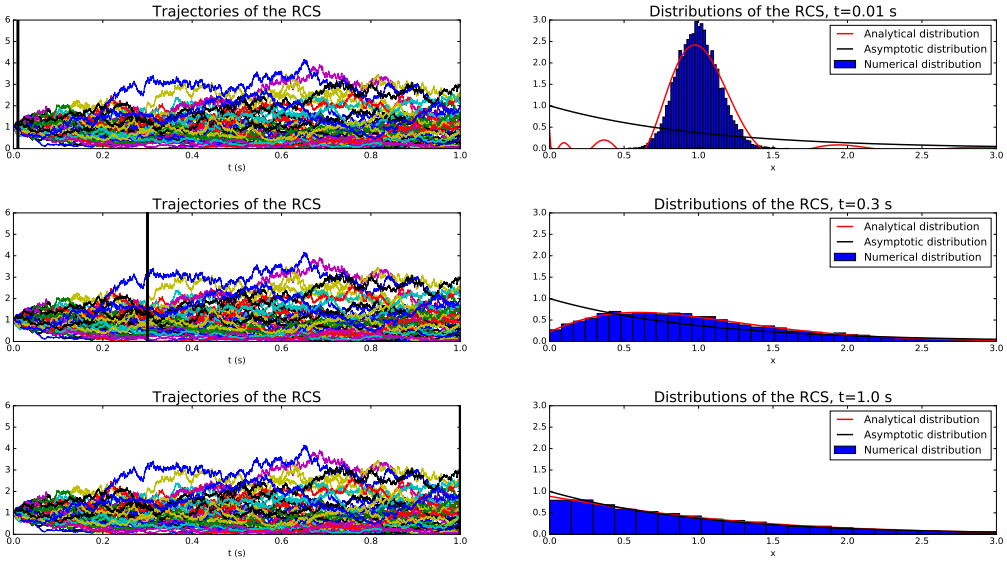

Figure 3. Comparison between analytical distributions of x_t derived from the resolution of the FPE, and numerical distributions derived from the resolutions of the SDE using the Milstein method. 10000 trajectories are computed with $\mathcal{A} = 1$ Hz, $\alpha = 1$ and $y = 1$.

3.3. *Distributions of the real (and imaginary) reflectivity*

We defined the in-phase and quadrature-phase components I_t and Q_t by $I_t = Re(\Psi_t) = x_t^{1/2}\gamma_t^{(R)}$ and $Q_t = Im(\Psi_t) = x_t^{1/2}\gamma_t^{(I)}$. Since $\gamma_t^{(R)}$ and $\gamma_t^{(I)}$ have the same distributions (for equal initial conditions), so will I_t and Q_t. Thus, it is sufficient to compute those of I_t. We remind that the processes $x_t^{1/2}$ and $\gamma_t^{(R)}$ are independent. In the following, we denote g the function $g : x \mapsto x^{1/2}$.

3.3.1. Stationary probability

From $x_\infty^{1/2} = g(x_\infty)$ and from equation (23) we get:

$$\begin{aligned} p(x_\infty^{1/2} = x) &= p(x_\infty = x^2) 2x \, \mathbf{1}_{[0,+\infty[}(x) \\ &= \frac{2\alpha^\alpha \, x^{2\alpha-1} \, e^{-\alpha x^2}}{\Gamma(\alpha)} \mathbf{1}_{[0,+\infty[}(x). \end{aligned} \tag{31}$$

We compute $p(I_\infty = x)$ as the distribution of the product of 2 independent random variables:

$$\begin{aligned} p(I_\infty = x) &= p\left(x_\infty^{1/2}\gamma_\infty^{(R)} = x\right) \\ &= \int_{\mathbb{R}^+} p(x_\infty^{1/2} = u)p\left(\gamma_\infty^{(R)} = x/u\right)\frac{1}{u}du \\ &= \frac{2\alpha^\alpha}{\sqrt{\pi}\Gamma(\alpha)}\int_{\mathbb{R}^+} u^{2\alpha-2}e^{-\left(\left(\frac{x}{u}\right)^2+\alpha u^2\right)}du. \end{aligned} \tag{32}$$

3.3.2. Transition probabilities

$I_t = x_t^{1/2}\gamma_t^{(R)}$ is the product of the square-root of the RCS and the speckle. We will show that we can compute $p\left(I_t = x|x_0 = y,\, \gamma_0^{(R)} = z\right)$ from the transition probabilities $p(\gamma_t^{(R)} = .\,|\gamma_0^{(R)} = .\,)$ and $p(x_t = .\,|x_0 = .\,)$. From $x_t^{1/2} = g(x_t)$ and from equation (30), we can compute the conditioned probability $p(x_t^{\frac{1}{2}} = x|x_0 = y)$. Indeed, we remind that transformations and conditioning are commutative. As a result, the conditioned probability $p(x_t^{1/2} = x|x_0 = y)$ is the probability of the transformation by the function g of a random variable of conditioned probability $p(x_t = x|x_0 = y)$:

$$\begin{aligned} p(x_t^{1/2} = x|x_0 = y) &= p(g(x_t) = x|x_0 = y) \\ &= p(x_t = x^2|x_0 = y)2x \\ &\Leftrightarrow \\ p(x_t^{1/2} = x|x_0 = y) &= \sum_{n=0}^{+\infty}\frac{2\alpha L_n^{\alpha-1}(\alpha y)n!}{\Gamma(n+\alpha)}e^{-\mathcal{A}nt}xe^{-\alpha x^2}(\alpha x^2)^{\alpha-1}L_n^{\alpha-1}(\alpha x^2)\mathbf{1}_{[0,+\infty[}(x) \end{aligned}$$

By independence of the processes x_t and $\gamma_t^{(R)}$ and from the properties of conditioned probabilities in the framework of absolute continuity:

$$\begin{aligned} p\left(x_t^{1/2} = x|x_0 = y,\, \gamma_0^{(R)} = z\right) &= \frac{p\left(x_t^{1/2} = x,\, x_0 = y,\, \gamma_0^{(R)} = z\right)}{p\left(x_0 = y,\, \gamma_0^{(R)} = z\right)} \\ &= \frac{p\left(x_t^{1/2} = x,\, x_0 = y\right)p\left(\gamma_0^{(R)} = z\right)}{p(x_0 = y)p\left(\gamma_0^{(R)} = z\right)} \\ &= \frac{p\left(x_t^{1/2} = x,\, x_0 = y\right)}{p(x_0 = y)} \\ &= p\left(x_t^{1/2} = x|x_0 = y\right) \end{aligned}$$

which is very intuitive. Similarly, $p\left(\gamma_t^{(R)} = x|x_0 = y,\, \gamma_0^{(R)} = z\right) = p\left(\gamma_t^{(R)} = x|\gamma_0^{(R)} = z\right)$. Again by commutativity of transformations and con-

ditioning, we can compute $p\left(x_t^{1/2}\gamma_t^{(R)} = x|x_0 = y,\, \gamma_0^{(R)} = z\right)$ as the distribution of the product of 2 independent random variables:

$$p\left(x_t^{1/2}\gamma_t^{(R)} = x|x_0 = y,\, \gamma_0^{(R)} = z\right) = \int_0^{+\infty} p\left(\gamma_t^{(R)} = x/u \mid x_0 = y,\, \gamma_0^{(R)} = z\right) p\left(x_t^{1/2} = u \mid x_0 = y,\, \gamma_0^{(R)} = z\right)\frac{1}{u}du$$

$\Leftrightarrow$

$$p\left(I_t = x \mid x_0 = y,\, \gamma_0^{(R)} = z\right) = \int_0^{+\infty} \frac{1}{\sqrt{2\pi v(t)}} e^{-\frac{1}{2}\frac{(\frac{x}{u}-m(t))^2}{v(t)}} \sum_{n=0}^{+\infty} \frac{2\alpha L_n^{\alpha-1}(\alpha y) n!}{\Gamma(n+\alpha)} e^{-\mathcal{A}nt} e^{-\alpha u^2} (\alpha u^2)^{\alpha-1} L_n^{\alpha-1}(\alpha u^2) du \tag{33}$$

where $m(t)$, $v(t)$ are expressed in equations (18) and (19) with z replacing y in the expression of $m(t)$. The mathematical details are provided in appendix A.1 and are based on relation (2) applied to the couple $(x_t^{1/2}, \gamma_t^{(R)})$.

Equation (33) is an exact analytical expression of the transition probabilities of I_t. It is explicit and relatively easy to evaluate numerically. As mentionned earlier, it is also valid for Q_t where the condition $\gamma_0^{(R)} = z$ is replaced by $\gamma_0^{(I)} = z$. Figure 4 shows the very good agreement between the analytical and numerical distributions. We solve numerically the SDE for $x_t, \gamma_t^{(R)}$ with Dirac initial conditions and then compute I_t with the relation $I_t = x_t^{1/2}\gamma_t^{(R)}$. As for x_t, oscillations appear for short times since the sum (30) must be truncated approximately at $n = 150$. We observe a difference between the transition probabilities of x_t and $\gamma_t^{(R)}$ on one side, and those of I_t on the other side. x_t was conditioned only by x_0 and $\gamma_t^{(R)}$ by $\gamma_0^{(R)}$, but I_t is conditioned by x_0 and $\gamma_0^{(R)}$, not just I_0. It is more constraining since $I_0 = x_0^{1/2}\gamma_0^{(R)}$. We observed numerically that the transition probabilities cannot depend only on I_0 but must depend on both x_0 and $\gamma_0^{(R)}$. For example, the conditions $x_0 = 1$, $\gamma_0^{(R)} = 2$ and $x_0 = 4$, $\gamma_0^{(R)} = 1$ give different transitional probabilities even though in both cases $I_0 = 2$. Physically, this is explained by the difference between the dynamics of the speckle and the RCS, which evolve on different timescales. The same remark holds in the next section for the intensity.

3.4. *Distributions of the intensity*

The intensity z_t is defined by $z_t = |\Psi_t|^2 = x_t\left(\gamma_t^{(R)\,2} + \gamma_t^{(I)\,2}\right)$. In this section, we derive its transition probabilities.

3.4.1. Stationary probability

The stationary distribution of the intensity is the classical K distribution as shown below. Equation (16) states that $\gamma_\infty^{(R)} \sim \gamma_\infty^{(I)} \sim \mathcal{N}(0, 1/2)$, *i.e.* $\sqrt{2}\gamma_\infty^{(R)} \sim \sqrt{2}\gamma_\infty^{(I)} \sim$

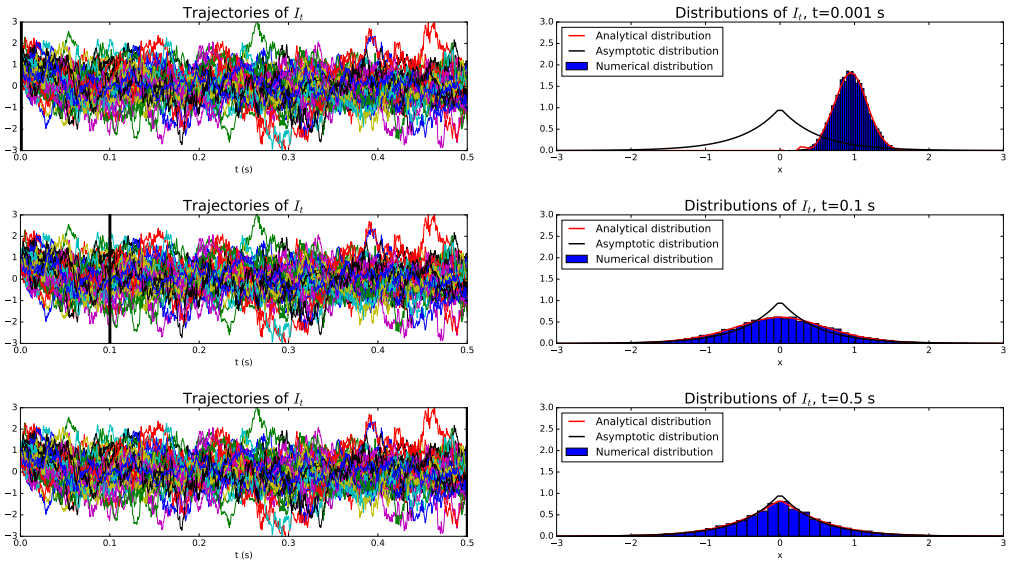

Figure 4. Comparison between analytical distributions of I_t (33) and numerical distributions. 10000 trajectories are computed with $\mathcal{A} = 1$ Hz, $\alpha = 1$, $\mathcal{B} = 100$ Hz, $x_0 = 1$ and $\gamma_0^{(R)} = 1$.

$\mathcal{N}(0,1)$. Since $\gamma_\infty^{(R)}$ and $\gamma_\infty^{(I)}$ are independent, $\sqrt{2}\gamma_\infty^{(R)\,2} + \sqrt{2}\gamma_\infty^{(I)\,2} \sim \chi_2^2$. We get:

$$\begin{aligned} p\left(\sqrt{2}\gamma_\infty^{(R)\,2} + \sqrt{2}\gamma_\infty^{(I)\,2} = x\right) &= \frac{1}{2}e^{-x/2} \\ \Leftrightarrow p\left(\gamma_\infty^{(R)\,2} + \gamma_\infty^{(I)\,2} = x\right) &= e^{-x} \end{aligned} \tag{34}$$

x_∞ and $\gamma_\infty^{(R)\,2} + \gamma_\infty^{(I)\,2}$ are independent (for physical reasons, see section 2.2) and their distributions are given respectively by equation (23) and equation (34). As the distribution of a product of 2 independent random variables, we get:

$$\begin{aligned} p(z_\infty = x) &= p\left(x_\infty\left(\gamma_\infty^{(R)\,2} + \gamma_\infty^{(I)\,2}\right) = x\right) \\ &= \int_{\mathbb{R}^+} p(x_\infty = u) p\left(\left(\gamma_\infty^{(R)\,2} + \gamma_\infty^{(I)\,2}\right) = \frac{x}{u}\right)\frac{1}{u}du \\ &= \int_{\mathbb{R}^+} \frac{\alpha(\alpha u)^{\alpha-1}e^{-\alpha u}}{\Gamma(\alpha)}\frac{e^{-x/u}}{u}du. \end{aligned}$$

Since $\frac{e^{-x/u}}{u} = p(z_\infty = x|x_\infty = u)$ ([4] p 103) and $\frac{\alpha(\alpha u)^{\alpha-1}e^{-\alpha u}}{\Gamma(\alpha)} = p(x_\infty = u)$ we get (see [4] p 109):

$$p(z_\infty = x) = \frac{2\alpha^{\frac{\alpha+1}{2}}x^{\frac{\alpha-1}{2}}}{\Gamma(\alpha)}K_{\alpha-1}(2\sqrt{\alpha x}), \tag{35}$$

where K is the modified Bessel function of the second kind.

3.4.2. Transition probabilities

We know from section 3.1 that $\forall x \in \mathbb{R}$, $\forall t > 0$:

$$\begin{cases} p\left(\gamma_t^{(R)} = x | \gamma_0^{(R)} = z\right) = \frac{1}{\sqrt{2\pi v(t)}} e^{-\frac{1}{2}\frac{(x-m_R(t))^2}{v(t)}} \\ p\left(\gamma_t^{(I)} = x | \gamma_0^{(I)} = w\right) = \frac{1}{\sqrt{2\pi v(t)}} e^{-\frac{1}{2}\frac{(x-m_I(t))^2}{v(t)}} \end{cases} \tag{36}$$

with:

$$\begin{cases} v(t) = \frac{1-e^{-\mathcal{B}t}}{2} \\ m_R(t) = ze^{-\frac{\mathcal{B}}{2}t} \\ m_I(t) = we^{-\frac{\mathcal{B}}{2}t}. \end{cases} \tag{37}$$

Let $X = \frac{1}{\sqrt{v(t)}} \begin{pmatrix} cond\left(\gamma_t^{(R)}\right) \\ cond\left(\gamma_t^{(I)}\right) \end{pmatrix}$ where $cond\left(\gamma_t^{(R)}\right)$ and $cond\left(\gamma_t^{(I)}\right)$ are independent random variables such that $p\left(cond\left(\gamma_t^{(R)}\right) = x\right) = p\left(\gamma_t^{(R)} = x | \gamma_0^{(R)} = z\right)$ and $p\left(cond\left(\gamma_t^{(I)}\right) = x\right) = p\left(\gamma_t^{(I)} = x | \gamma_0^{(I)} = z\right)$. Then $\mathbb{E}[X] = \frac{1}{\sqrt{v(t)}} \begin{pmatrix} m_R(t) \\ m_I(t) \end{pmatrix}$ and from the independance of $cond\left(\gamma_t^{(R)}\right)$ and $cond\left(\gamma_t^{(I)}\right)$, $\Gamma_X = \begin{bmatrix} 1 & 0 \\ 0 & 1 \end{bmatrix}$ where Γ_X is the covariance matrix of X. We apply theorem 1.3.4 p 22 of [17], with $n = 2$ and a non-centrality coefficient δ:

$$\begin{aligned} \delta(t) &= \frac{1}{\sqrt{v(t)}} \begin{pmatrix} m_R(t) & m_I(t) \end{pmatrix} \frac{1}{\sqrt{v(t)}} \begin{pmatrix} m_R(t) \\ m_I(t) \end{pmatrix} \\ &= \frac{1}{v(t)} (m_R(t)^2 + m_I(t)^2) \\ &= \frac{2e^{-\mathcal{B}t}(z^2 + w^2)}{1 - e^{-\mathcal{B}t}}. \end{aligned}$$

We obtain:

$$p\left(\frac{1}{v(t)}\left(cond\left(\gamma_t^{(R)}\right)^2 + cond\left(\gamma_t^{(I)}\right)^2\right) = x\right) = \frac{1}{2} e^{-\frac{x+\delta(t)}{2}} {}_0F_1\left(1, \frac{1}{4}\delta(t)x\right).$$

We can express this result with the modified Bessel function of the first kind $\mathcal{I}_0$ defined as:

$$\mathcal{I}_0(z) = \sum_{n=0}^{+\infty} \frac{\left(\frac{1}{4}z^2\right)^n}{n!\Gamma(n+1)}.$$

Upon replacing $z = \sqrt{\delta(t)x}$ we get:

$$I_0(\sqrt{\delta(t)x}) = \sum_{n=0}^{+\infty} \frac{\left(\frac{1}{4}\delta(t)x\right)^n}{n!^2} = {}_0F_1\left(1, \frac{1}{4}\delta(t)x\right)$$

such that

$$p\left(\frac{1}{v(t)}\left(cond\left(\gamma_t^{(R)}\right)^2+cond\left(\gamma_t^{(I)}\right)^2\right)=x\right)=\frac{1}{2}e^{-\frac{x+\delta(t)}{2}}I_0\left(\sqrt{\delta(t)x}\right).$$

Let g be the function:

$$\begin{aligned} g:\mathbb{R}&\to\mathbb{R}\\ x&\mapsto v(t)x \end{aligned}$$

We have $cond\left(\gamma_t^{(R)}\right)^2+cond\left(\gamma_t^{(I)}\right)^2=g\left(\frac{1}{v(t)}\left(cond\left(\gamma_t^{(R)}\right)^2+cond\left(\gamma_t^{(I)}\right)^2\right)\right)$ and we obtain:

$$p\left(cond\left(\gamma_t\right)^2=x\right)=\frac{1}{2v(t)}e^{-\frac{\frac{x}{v(t)}+\delta(t)}{2}}I_0\left(\sqrt{\frac{\delta(t)x}{v(t)}}\right),$$

with $cond\left(\gamma_t\right)^2=cond\left(\gamma_t^{(R)}\right)^2+cond\left(\gamma_t^{(I)}\right)^2$. We also introduce the notation $\gamma_t^2=\gamma_t^{(R)\,2}+\gamma_t^{(I)\,2}$.

We define $cond(x_t)$ as a random variable such that $p(cond(x_t)=x)=p(x_t=x|x_0=y)$, for example solution to (13) with a Dirac-distributed initial condition. $cond(x_t)$ and $cond\left(\gamma_t\right)^2$ are independent, from what we get:

$$p\left(cond\left(x_t\right)cond\left(\gamma_t\right)^2=x\right)=\int_0^{+\infty}p\left(cond\left(\gamma_t\right)^2=x/u\right)p\left(x_t=u\right)\frac{1}{u}du$$

$\Leftrightarrow$

$$\begin{aligned} p\left(z_t=x|x_0=y,\,\gamma_0^{(R)}=z,\,\gamma_0^{(I)}=w\right)=\int_0^{+\infty}&\frac{1}{2v(t)}e^{-\frac{\frac{x}{v(t)u}+\delta(t)}{2}}I_0\left(\sqrt{\frac{\delta(t)x}{v(t)u}}\right)\\ &\sum_{n=0}^{+\infty}\frac{\alpha L_n^{\alpha-1}(\alpha y)n!}{\Gamma(n+\alpha)}e^{-\mathcal{A}nt}e^{-\alpha u}(\alpha u)^{\alpha-1}L_n^{\alpha-1}(\alpha u)\frac{1}{u}du \end{aligned} \tag{38}$$

We obtained equation (38) by application of transformations to conditioned random variables, which is equivalent to conditioning the transformed random variables, according to relation (2). We will not provide the full details since we want to maintain the focus on the results. The proof is similar to that for the real (and imaginary) reflectivity in appendix A.1. Equation (38) yields the distribution of z_t conditioned by the measure $x_0=y$, $\gamma_0^{(R)}=z$; $\gamma_0^{(I)}=w$. However, the knowledge of both $\gamma_t^{(R)}$ and $\gamma_t^{(I)}$ is not necessary. z and w take part in the expression of $\delta(t)$ only, in which only the value z^2+w^2 must be known. Consequently, one can state

that

$$p\left(z_t = x|x_0 = y,\, \gamma_0^{(R)\,2} + \gamma_0^{(I)\,2} = u\right) = \int_0^{+\infty} \frac{1}{2v(t)} e^{-\frac{\frac{x}{v(t)u}+\delta(t)}{2}} I_0\left(\sqrt{\frac{\delta(t)x}{v(t)u}}\right) \sum_{n=0}^{+\infty} \frac{\alpha L_n^{\alpha-1}(\alpha y) n!}{\Gamma(n+\alpha)} e^{-\mathcal{A}nt} e^{-\alpha u} (\alpha u)^{\alpha-1} L_n^{\alpha-1}(\alpha u) \frac{1}{u} du \tag{39}$$

where $u = z^2 + w^2$. Equation (39) is an exact analytical expression of the distribution of z_t which is explicit and relatively easy to evaluate numerically. Assuming that the RCS is constant, we get $x_t = 1$ or $p(x_t = x) = \delta_1(x)$. Replacing this expression in (39) gives after calculations:

$$\begin{aligned} p(z_t = x|x_t = s) &= \frac{1}{(1-e^{-\mathcal{B}t})s} e^{-\frac{x+z_0 e^{-\mathcal{B}t}}{(1-e^{-\mathcal{B}t})s}} I_0\left(\sqrt{\frac{4e^{-\mathcal{B}t} z_0 x}{(1-e^{-\mathcal{B}t})^2 s^2}}\right) \\ &= \frac{1}{(1-e^{-\mathcal{B}t})s}\; e^{-\frac{x+z_0 e^{-\mathcal{B}t}}{(1-e^{-\mathcal{B}t})s}}\; I_0\left(\frac{2e^{-\mathcal{B}\frac{t}{2}}}{(1-e^{-\mathcal{B}t})s}\sqrt{x z_0}\right) \end{aligned}$$

which is formula 8.53 p 63 of [3]. Equation (39) is therefore a generalization of this formula for RCS varying in time according to Field's model (12).

Figure 5 represents numerical trajectories of the intensity. We simulated trajectories of x_t using the Miltein method and trajectories of $\gamma_t^{(R)}$ and $\gamma_t^{(I)}$ using the Euler-Maruyama method. The intensity was then computed using the relation $z_t = x_t\left(\gamma_t^{(R)\,2} + \gamma_t^{(I)\,2}\right) = x_t\gamma_t^2$. The initial conditions were: $x_0 = 1$, $\gamma_0^{(R)} = 1$, $\gamma_0^{(I)} = 1$, *i.e.* $z_0 = 2$. There is a very good agreement between formula (39) and numerical distributions. The distribution is almost centered around $x = 2$ at $t = 0.001$ s and then progressively converges toward the asymptotic K distribution (formula (35)). As for x_t, I_t, Q_t, oscillations appear for short times since the sum in equation (30) must be truncated approximately at $n = 150$.

4. Present to past transition probabilities

At the stage we have reached, we are able to perform forward probabilistic predictions (present to future) for $x_t, \gamma_t^{(R)}, \gamma_t^{(I)}, I_t, Q_t, z_t$. Let X_t denote any of these and assume that a measure $\tilde{X}_t = x$ is made at time t. In section 3, we derived forward conditioned probabilities of the type $p(X_t = x|X_0 = y)$ for the RCS and speckle, and $p(X_t = x|Y_0 = y,\, Z_0 = z)$ for the real (and imaginary) reflectivity and the intensity. To answer the question "what was the value of X_{t-h} knowing that $X_t = x$ or that $Y_t = y$, $Z_t = z$?", we must reverse the conditions to obtain $p(X_{t-h} = y|X_t = y)$ or $p(X_{t-h} = x|Y_t = y,\, Z_t = z)$, the distribution of X_{t-h} conditioned by measures located in the future relative to $t - h$. The resulting distributions can be used to make backward probabilistic inferences (present to past). In the remaining of this section, we treat the RCS and speckle together and the real (and imaginary) reflectivity and the intensity in two different sections.

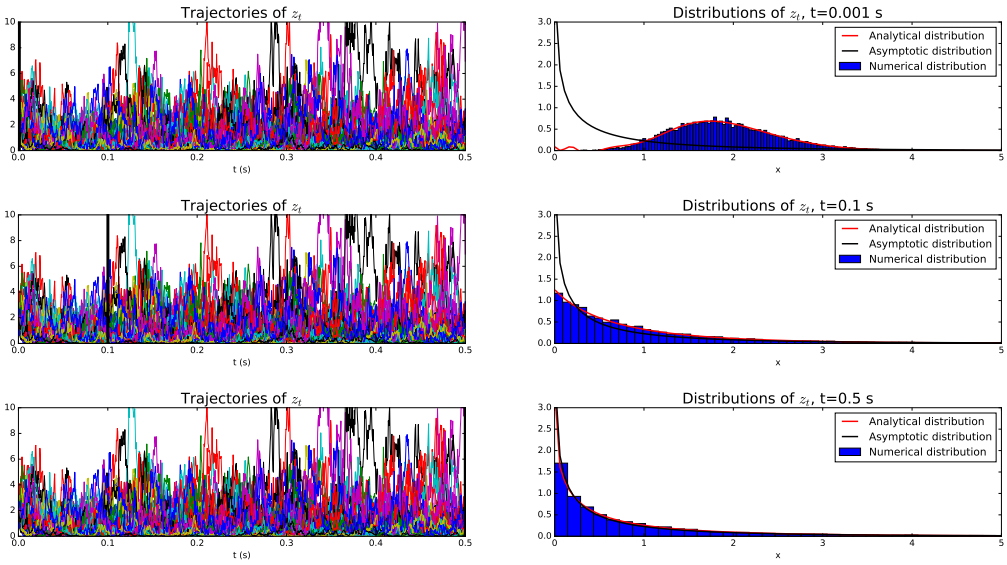

Figure 5. Comparison between analytical distributions of z_t (39) and numerical distributions. 10000 trajectories are computed with $\mathcal{A} = 1$ Hz, $\alpha = 1$, $\mathcal{B} = 100$ Hz, $x_0 = 1$, $\gamma_0^{(R)} = 1$, $\gamma_0^{(I)} = 1$.

4.1. *Distributions of the speckle and RCS*

Reversing the present to future probabilities for the speckle, equation (17), and for the RCS, equation (30), is straightforward as shown below. Let X_t denote either the speckle or the RCS. We can write the transition probabilities in the following way:

$$p(X_{t-h} = y | X_t = x) = \frac{p(X_t = x,\, X_{t-h} = y)}{p(X_t = x)} = \frac{p(X_t = x | X_{t-h} = y) p(X_{t-h} = y)}{p(X_t = x)}$$
$$\Leftrightarrow p(X_{t-h} = y | X_t = x) = \frac{p(X_t = x | X_{t-h} = y) p(X_\infty = y)}{p(X_\infty = x)} \tag{40}$$

We have used absolute continuity and the fact that the physical process (see section 2.1) is asymptotically distributed at any time t.

In the case of the speckle, the asymptotic distribution is given by formula (16) from which:

$$\frac{p(\gamma_\infty^{(R)} = y)}{p(\gamma_\infty^{(R)} = x)} = e^{-(y^2 - x^2)}.$$

We also remind that by homogeneity of the Markov process $\gamma_t^{(R)}$, $p(\gamma_t^{(R)} = x | \gamma_{t-h}^{(R)} = y) = p(\gamma_h^{(R)} = x | \gamma_0^{(R)} = y) = \frac{1}{\sqrt{2\pi v(h)}} e^{-\frac{1}{2}\frac{(x - m(h))^2}{v(h)}}$ with $v(h) = \frac{1 - e^{-\mathcal{B}h}}{2}$ and $m(h) =$

$ye^{-\mathcal{B}t/2}$. After some calculations, we can show that:

$$\begin{aligned} p(\gamma_{t-h}^{(R)} = y|\gamma_t^{(R)} = x) &= \frac{1}{\sqrt{2\pi v(h)}} e^{-\frac{1}{2}\frac{(x-ye^{-\mathcal{B}t/2})^2}{v(h)}} e^{-(y^2-x^2)} \\ &= \frac{1}{\sqrt{2\pi v(h)}} e^{-\frac{1}{2}\frac{(y-xe^{-\mathcal{B}t/2})^2}{v(h)}} \\ \Leftrightarrow p(\gamma_{t-h}^{(R)} = y|\gamma_t^{(R)} = x) &= p(\gamma_h^{(R)} = y|\gamma_0^{(R)} = x). \end{aligned} \tag{41}$$

In the case of the RCS, the asymptotic distribution is given by formula (23) from which:

$$\frac{p(x_\infty = y)}{p(x_\infty = x)} = \left(\frac{y}{x}\right)^{\alpha-1} e^{-\alpha(y-x)}.$$

Using the forward transition probabilities (30) and the homogeneity of the process x_t, we obtain:

$$\begin{aligned} p(x_{t-h} = y|x_t = x) &= \sum_{n=0}^{+\infty} \frac{\alpha L_n^{\alpha-1}(\alpha y) n!}{\Gamma(n+\alpha)} e^{-\mathcal{A}nt} e^{-\alpha x} \left(\frac{\alpha xy}{x}\right)^{\alpha-1} L_n^{\alpha-1}(\alpha x) e^{-\alpha(y-x)} \\ &= \sum_{n=0}^{+\infty} \frac{\alpha L_n^{\alpha-1}(\alpha x) n!}{\Gamma(n+\alpha)} e^{-\mathcal{A}nt} e^{-\alpha y} (\alpha y)^{\alpha-1} L_n^{\alpha-1}(\alpha y) \\ \Leftrightarrow p(x_{t-h} = y|x_t = x) &= p(x_h = y|x_0 = x) \end{aligned} \tag{42}$$

Formula (41) and (42) show that for the speckle and the RCS, the same formula hold for backward and forward probabilistic inferences.

4.2. *Distributions of the real (and imaginary) reflectivity*

In section 3.3, we have obtained the distribution of I_h conditioned by ($x_0 = y$, $\gamma_0^{(R)} = z$), which is the same as the distribution of I_t conditioned by ($x_{t-h} = y$, $\gamma_{t-h}^{(R)} = z$). We would like to obtain the distribution of I_{t-h} conditioned by ($x_t = y$, $\gamma_t^{(R)} = z$). To do so, we first reverse the conditioning of the couple $\left(x_t, \gamma_t^{(R)}\right)$:

$$\begin{aligned} p\left(x_t = z, \gamma_t^{(R)} = w|x_{t-h} = x, \gamma_{t-h}^{(R)} = y\right) &= \frac{p\left(x_t = z, x_{t-h} = x, \gamma_t^{(R)} = w, \gamma_{t-h}^{(R)} = y\right)}{p\left(x_{t-h} = x, \gamma_{t-h}^{(R)} = y\right)} \\ &= \frac{p\left(x_t = z, x_{t-h} = x\right) p\left(\gamma_t^{(R)} = w, \gamma_{t-h}^{(R)} = y\right)}{p(x_{t-h} = x) p\left(\gamma_{t-h}^{(R)} = y\right)} \\ &= p(x_t = z|x_{t-h} = x) p\left(\gamma_t^{(R)} = w|\gamma_{t-h}^{(R)} = y\right). \end{aligned}$$

We have used the independence of the processes x_t and $\gamma_t^{(R)}$ in the second equality. Similarly, we can show that:

$$p\left(x_{t-h}=z,\,\gamma_{t-h}^{(R)}=w|x_t=x,\,\gamma_t^{(R)}=y\right)=p(x_{t-h}=z|x_t=x)p\left(\gamma_{t-h}^{(R)}=w|\gamma_t^{(R)}=y\right).$$

Since $p(x_{t-h}=z|x_t=x)=p(x_h=z|x_0=x)=p(x_t=z|x_{t-h}=x)$ and $p\left(\gamma_{t-h}^{(R)}=w|\gamma_t^{(R)}=y\right)=p\left(\gamma_t^{(R)}=w|\gamma_{t-h}^{(R)}=y\right)$, we get:

$$p\left(x_{t-h}=z,\,\gamma_{t-h}^{(R)}=w|x_t=x,\,\gamma_t^{(R)}=y\right)=p\left(x_t=z,\,\gamma_t^{(R)}=w|x_{t-h}=x,\,\gamma_{t-h}^{(R)}=y\right). \tag{43}$$

The relation (43) is similar to relations (41) and (42) for the couple $\left(x_t,\gamma_t^{(R)}\right)$ seen as a $\mathbb{R}^2-$valued process. By commutativity of C^1-diffeomorphisms and conditioning, $p\left(I_{t-h}=z|x_t=x,\,\gamma_t^{(R)}=y\right)$ is obtained as the distribution of the appropriate transformation (see section 3.3) applied to the couple $\left(x_{t-h},\gamma_{t-h}^{(R)}\right)$ conditioned by $\left(x_t=x,\,\gamma_t^{(R)}=y\right)$, which has the conditioned distribution $p\left(x_{t-h}=z,\,\gamma_{t-h}^{(R)}=w|x_t=x,\,\gamma_t^{(R)}=y\right)$. From formula (43), we obtain exactly the same result as we did in section 3.3:

$$p\left(I_{t-h}=x|x_t=y,\,\gamma_t^{(R)}=z\right)=p\left(I_h=x|x_0=y,\,\gamma_0^{(R)}=z\right) \tag{44}$$

Formula (44) along with formula (33) enables backward probabilistic inferences of the real (and imaginary) reflectivity.

4.3. *Distributions of the intensity*

In section 3.4, we have obtained the distribution of z_h conditioned by $(x_0=y,\,\gamma_0^{(R)\,2}+\gamma_0^{(I)\,2}=u)$, which is the same as the distribution of z_t conditioned by $\left(x_{t-h}=y,\,\gamma_{t-h}^{(R)\,2}+\gamma_{t-h}^{(I)\,2}=u\right)$ by homogeneity. We would like to obtain the distribution of z_{t-h} conditioned by $(x_t=y,\,\gamma_t^{(R)\,2}+\gamma_t^{(I)\,2}=u)$. To do so, we reverse the conditioning of the random vector $\left(x_t,\gamma_t^{(R)},\gamma_t^{(I)}\right)$. By mutual independence of x_t, $\gamma_t^{(R)}$ and $\gamma_t^{(I)}$, we can show that:

$$\begin{aligned}
&p\left(x_t=x,\gamma_t^{(R)}=y,\gamma_t^{(I)}=z|x_{t-h}=u,\gamma_{t-h}^{(R)}=v,\gamma_{t-h}^{(I)}=w\right)\\
&=p(x_t=x|x_{t-h}=u)p\left(\gamma_t^{(R)}=y|\gamma_{t-h}^{(R)}=v\right)p\left(\gamma_t^{(I)}=z|\gamma_{t-h}^{(I)}=w\right)\\
&=p(x_{t-h}=x|x_t=u)p\left(\gamma_{t-h}^{(R)}=y|\gamma_t^{(R)}=v\right)p\left(\gamma_{t-h}^{(I)}=z|\gamma_t^{(I)}=w\right)\\
&=p\left(x_{t-h}=x,\gamma_{t-h}^{(R)}=y,\gamma_{t-h}^{(I)}=z|x_t=u,\gamma_t^{(R)}=v,\gamma_t^{(I)}=w\right)
\end{aligned} \tag{45}$$

Formula (39) resulted from transformations that implicitely led from $p\left(x_t=.\,,\gamma_t^{(R)}=.\,,\gamma_t^{(I)}=.\,|x_{t-h}=y,\gamma_{t-h}^{(R)}=z,\gamma_{t-h}^{(I)}=w\right)$ to $p\left(x_t\left(\gamma_t^{(R)\,2}+\gamma_t^{(I)\,2}\right)=.\,|x_{t-h}=y,\gamma_{t-h}^{(R)\,2}+\gamma_{t-h}^{(I)\,2}=u\right)$. It is

not explicit since the transformations were applied to the marginal distributions $p\left(x_t = . \,|x_{t-h} = y, \gamma_{t-h}^{(R)} = z, \gamma_{t-h}^{(I)} = w\right)$, $p\left(\gamma_t^{(R)} = . \,|x_{t-h} = y, \gamma_{t-h}^{(R)} = z, \gamma_{t-h}^{(I)} = w\right)$ etc. This approach was justified by the commutativity between conditioning and transformations.

Similarly, the distribution $p\left(x_{t-h}\left(\gamma_{t-h}^{(R)\,2} + \gamma_{t-h}^{(I)\,2}\right) = . \,|x_t = y, \gamma_t^{(R)\,2} + \gamma_t^{(I)\,2} = u\right)$ will be obtained from the same transformations applied to $p\left(x_{t-h} = . \,, \gamma_{t-h}^{(R)} = . \,, \gamma_{t-h}^{(I)} = . \,|x_t = u, \gamma_t^{(R)} = v, \gamma_t^{(I)} = w\right)$. Using equation (45) and the homogeneity of the intensity, we get a relation similar to formula (41), (42) and (44) for the intensity:

$$p\left(z_{t-h} = x|x_t = y, \gamma_t^{(R)\,2} + \gamma_t^{(I)\,2} = u\right) = p\left(z_h = x|x_0 = y, \gamma_0^{(R)\,2} + \gamma_0^{(I)\,2} = u\right). \tag{46}$$

Formula (46) along with formula (39) enables backward probabilistic inferences of the intensity.

5. Discussion

From sections (3) and (4) we know how to perform forward and backward probabilistic inferences for $\gamma_t^{(R)}, \gamma_t^{(I)}, x_t, I_t, Q_t, z_t$. We have left aside a few comments that we address here. Formula (17), (30), (33), (39) are for forward probabilistic inferences. We remind that the processes at stake here are all homogeneous Markov processes: the formula apply to any forward leap no matter the starting time. Formula (41), (42), (44) and (46) are for backward probabilistic inferences. They are directly expressed for any starting time t, for a backward leap of length h. It was assumed that we can actually measure the starting values in practice. Measuring it gives a condition $X_t = y$ that we can project forward to time X_{t+h} or backward to time X_{t-h}, with $h > 0$. The assumption is justified: the radar which observes the sea surface records a time series of the complex-valued reflectivity Ψ_t. Taking the real and imaginary parts respectively gives I_t and Q_t, and taking the squared-modulus gives z_t. The phase θ_t can also directly be obtained by taking an argument of Ψ_t. On the contrary, the RCS x_t is not directly observed. However Fayard and Field provide formula to optimally infer it from increments of z_t and of the phase θ_t [18]. Once the time series of x_t has been obtaining from this algorithm, $\gamma_t^{(R)}$ and $\gamma_t^{(I)}$ can be computed from $\gamma_t^{(R)} = \frac{I_t}{x_t^{1/2}}$ and $\gamma_t^{(I)} = \frac{Q_t}{x_t^{1/2}}$. [18] is thus the key for making our formula effectivily usable.

Figure 6 represents schematically a discrete time series of values of the RCS (for example) measured by a moving sensor (or different sensors) from positions u_1, u_2, u_3, u_4, u_5 at times t_1, t_2, t_3, t_4, t_5. To be compared, these measures must be transported to the same common time, chosen to be $t = 0.25$ s here, *i.e.* the time at which the central measure $\tilde{X}_{t_3}^{(u_3)}$ has been taken. The measures $\tilde{X}_{t_1}^{(u_1)}$ and $\tilde{X}_{t_2}^{(u_2)}$ are projected forward using formula (30). The projection of $\tilde{X}_{t_1}^{(u_1)}$ at time $t_1 + h$ can be seen as a random variable with the distribution $p\left(X_{t_1+h}^{(u_1)} = . \,|X_{t_1}^{(u_1)} = \tilde{X}_{t_1}^{(u_1)}\right)$, which has an increasing variance with h has seen for example in figure 3. This is represented in figure 6 by the two solid blue line diverging from $\tilde{X}_{t_1}^{(u_1)}$. The variance

increases until it reaches a maximum value of $1/\alpha$ for $h = +\infty$ (see formula (23) of the asymptotic distribution). The expectation converges toward 1 as $h \to +\infty$. Those are asymptotic values which are not reached if h is not too large. We saw in figure 3 that for $A = 1$ Hz and $\alpha = 1$, the asymptotic distribution is not reached for $h = 0.25$ s but it is reached for $h = 0.5$ s. In the example of figure 6, the projection of the deterministic measure $\tilde{X}_{t_1}^{(u_1)}$ at the time reference $t = 0.25$ s is a random variable with the distribution $p\left(X_{t_1+0.25}^{(u_1)} = . \,|X_{t_1}^{(u_1)} = \tilde{X}_{t_1}^{(u_1)}\right)$, whose variance is smaller than the asymptotic variance $1/\alpha = 1$ and expectation different from the asymptotic expectation 1. This distribution is our best guess of what the measure of the RCS from position u_1 at the reference time t_3 would be. In the same way, projecting forward $\tilde{X}_{t_2}^{(u_2)}$ to the time $t_3 = 0.25$ s would give a distribution which would be our best guess of what the measure of the RCS from position u_2 would be at the reference time t_3. The above explanations apply as well for backward projection. Backward projection of the measures $\tilde{X}_{t_4}^{(u_4)}$ and $\tilde{X}_{t_5}^{(u_5)}$ are made using formula (42). For example, the measure $\tilde{X}_{t_5}^{(u_5)}$ projected backward by a timestep h gives the distribution $p\left(X_{t_5-h}^{(u_5)} = . \,|X_{t_5}^{(u_5)} = \tilde{X}_{t_5}^{(u_5)}\right)$, whose variance is again increasing with h. We wish to emphasize two points. Firstly, each of the random processes $X_t^{(u_i)}$ for $i = \{1, 2, 3, 4, 5\}$ is the RCS observed from a different position. If they are normalized by their mean value, such as in Field's model, equations (30) and (42) are applicable to any of them. Secondly, if the projection of a measure is not too far forward or backward, the result of the projection is a distribution different from the asymptotic (stationary) distribution, which is that of the unconditioned random variable $X_t^{(u_i)}$ for any i and t. The time series of deterministic measures $\{\tilde{X}_{t_1}^{(u_1)}, \tilde{X}_{t_2}^{(u_2)}, \tilde{X}_{t_3}^{(u_3)}, \tilde{X}_{t_4}^{(u_4)}, \tilde{X}_{t_5}^{(u_5)}\}$ transforms by projection to the reference time t_3 into a series of random variables $\{\hat{X}_{t_3}^{(u_1)}, \hat{X}_{t_3}^{(u_2)}, \hat{X}_{t_3}^{(u_3)}, \hat{X}_{t_3}^{(u_4)}, \hat{X}_{t_3}^{(u_5)}\}$ where $\hat{X}_{t_3}^{(u_i)}$ is the projection of $\tilde{X}_{t_1}^{(u_1)}$ at time t_3. Of course here, $\hat{X}_{t_3}^{(u_3)} = \tilde{X}_{t_3}^{(u_3)}$. The series of deterministic measures from different positions and times transformed into a series of probabilistic measure (random variables) from different positions at the same time.

6. Conclusions

This paper gives mathematical expressions for the forward and backward transition probabilities of the sea surface speckle, the RCS (texture), the real and imaginary parts of the reflectivity and intensity. We solved the Fokker-Planck equations of the speckle and RCS to obtain their transition probabilities (formula (17) and (30)), from which we computed those of the real and imaginary parts of the reflectivity and the intensity (formula (33) and (39)). Numerical simulations systematically reveal an accurate fit between the analytical and numerical distributions. They also illustrate how the initial deterministic measure progressively transforms into an asymptotically distributed random variable with increasing time (see sections 3).Using the rules of calculus of conditioned probabilities, we reversed the conditioning to obtain backward transition probabilities: formula (41), (42), (44), (46).

A series of deterministic measures of the complex reflectivity from different positions and times can then be processed to get a series of probabilistic measures of the speckle, RCS, real (and imaginary) reflectivity and intensity from different positions at the same time.

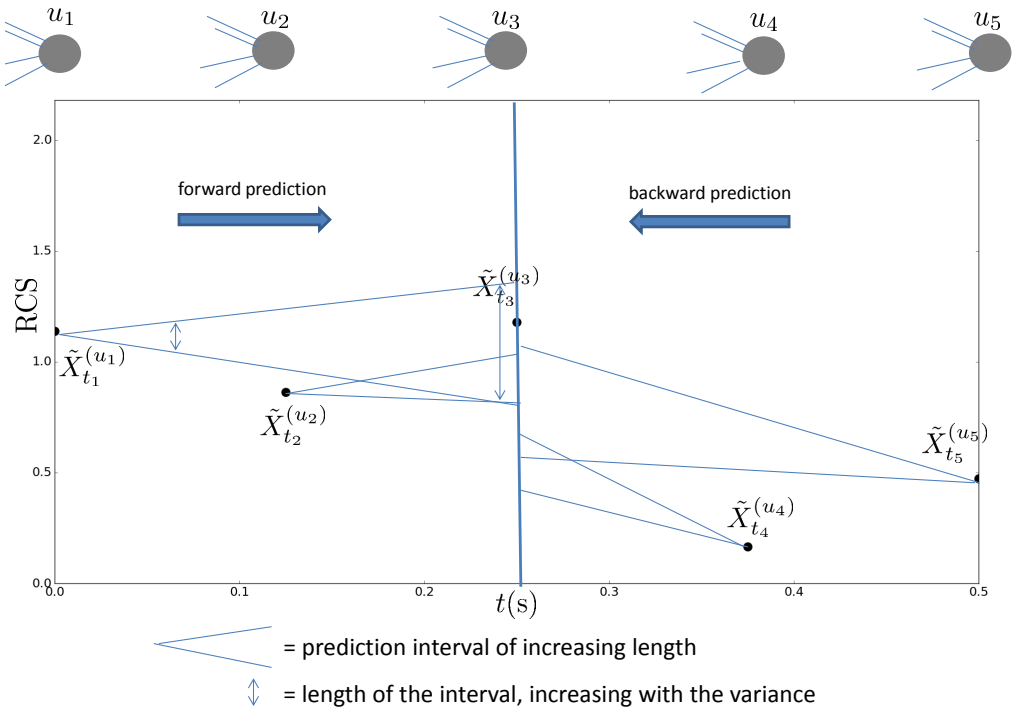

Figure 6. Forward and backward inferences of x_t to the common time $t = 0.25$ s.

All of these formula depend on 3 parameters which originally control the SDE of the RCS and the speckle and have not been estimated yet: $\alpha, \mathcal{A}$ and $\mathcal{B}$. We will work in the future on the estimation of these parameters as a function of the sea state. We continue to develop the applications of the results presented in this article in the field of radar imagery of the sea surface.

Appendix A. Complements

A.1. *Computational details for the forward transition probability of the real (and imaginary) reflectivity*

We know that $p\left(x_t^{\frac{1}{2}} = .|x_0 = x\right) = p\left(x_t^{\frac{1}{2}} = .|x_0 = x,\, \gamma_0^{(R)} = y\right)$ and that $p\left(\gamma_t^{(R)} = .|\gamma_0^{(R)} = y\right) = p\left(\gamma_t^{(R)} = .|x_0 = x,\, \gamma_0^{(R)} = y\right)$. We would like to compute $p\left(x_t^{\frac{1}{2}}\gamma_t^{(R)} = .|x_0 = x,\, \gamma_0^{(R)} = y\right)$. We show in section 4.2 that:

$$p\left(x_t^{\frac{1}{2}} = z,\, \gamma_t^{(R)} = w|x_0 = x,\, \gamma_0^{(R)} = y\right) = p\left(x_t^{\frac{1}{2}} = z|x_0 = x\right) p\left(\gamma_t^{(R)} = w|\gamma_0^{(R)} = y\right)$$

Let G be the C^1-diffeomorphism:

$$\begin{aligned} G: \quad \mathbb{R}^2 &\to \mathbb{R}^2 \\ (x, y) &\mapsto (xy, x) \end{aligned}$$

Let $cond\left(x_t^{\frac{1}{2}}, \gamma_t^{(R)}\right) = \left(cond\left(x_t^{\frac{1}{2}}\right), cond\left(\gamma_t^{(R)}\right)\right)$ be a random vector with the distibution:

$$p\left(cond\left(x_t^{\frac{1}{2}}, \gamma_t^{(R)}\right) = (z, w)\right) = p\left(x_t^{\frac{1}{2}} = z,\, \gamma_t^{(R)} = w | x_0 = x,\, \gamma_0^{(R)} = y\right)$$

We can show easily by integration that $cond\left(x_t^{\frac{1}{2}}\right)$ is a random variable with distribution $p\left(cond\left(x_t^{\frac{1}{2}}\right) = z\right) = p\left(x_t^{\frac{1}{2}} = z | x_0 = x\right)$ and that $cond\left(\gamma_t^{(R)}\right)$ is a random variable with distribution $p\left(cond\left(\gamma_t^{(R)}\right) = w\right) = p\left(\gamma_t^{(R)} = w | \gamma_0^{(R)} = y\right)$. Moreover, $cond\left(x_t^{\frac{1}{2}}\right)$ and $cond\left(\gamma_t^{(R)}\right)$ are independent.

From the commutativity relation (2), we get:

$$p\left(\left(x_t^{\frac{1}{2}}\gamma_t^{(R)},\, x_t^{\frac{1}{2}}\right) = (u, v) | x_0 = x,\, \gamma_0^{(R)} = y\right) = p\left(\left(cond\left(x_t^{\frac{1}{2}}\right) cond\left(\gamma_t^{(R)}\right)\right) = (u, v)\right),$$

and by integration:

$$p\left(x_t^{\frac{1}{2}}\gamma_t^{(R)} = u | x_0 = x,\, \gamma_0^{(R)} = y\right) = p\left(cond\left(x_t^{\frac{1}{2}}\right) cond\left(\gamma_t^{(R)}\right) = u\right). \qquad \text{(A1)}$$

This last equation together with the independance of $cond\left(x_t^{\frac{1}{2}}\right)$ and $cond\left(\gamma_t^{(R)}\right)$ and the knowledge of their distribution justifies the computations to obtain formula (33).

A.2. *Numerical resolution of SDE*

A SDE presents itself in the following form:

$$\mathrm{d}X_t = \mu(X_t, t)\mathrm{d}t + \sigma(X_t, t)\mathrm{d}W_t,$$

where $(W_t)_t$ is a brownian motion, also called Wiener process. μ is called the 'drift' and σ is called the 'volatility'. Understanding the algorithm for solving numerically this SDE is a very good way to gain intuitive understanding of its meaning. For precise definitions, refer to [12] for example. For what follows, refer to introduction to numerical simulation of SDE [19]. Let $[0, T]$ be a finite time interval and $t_0 = 0 < t_1 < ... < t_n$ a partition of $[0, T]$. The Euler-Maruyama method reads:

$$X_{t_i} = X_{t_{i-1}} + \mu(X_{t_{i-1}})(t_i - t_{i-1}) + \sigma(X_{t_{i-1}})(W_{t_i} - W_{t_{i-1}}), \qquad \text{(A2)}$$

Equation (A2) states that the increment of X between t_{i-1} and t_i is the sum of a term proportional to $t_i - t_{i-1}$ and a term proportional to the increment of the brownian motion $\Delta W_{t_i} = W_{t_i} - W_{t_{i-1}}$. This increment is a gaussian random variable with law $\mathcal{N}(0, t_i - t_{i-1})$. Generating a series of n random increments using Python for example leads to one possible trajectory. If many more increment series are generated, we can generate and visualize almost all possible trajectories and evaluate a numerical distribution of X_{t_i} for $i = 0...n$. We also use the slightly more elaborate Mistein's method (see [19]) when necessary.

A.3. *The Fokker-Planck equation*

Let us consider a SDE:

$$\mathrm{dX_t} = \mu(\mathrm{X_t})\mathrm{dt} + \sigma(\mathrm{X_t})\mathrm{dW_t}.$$

The Fokker-Planck equation associated with it is the partial differential equation (PDE), a.k.a 'Kolmogorov forward equation' [8]:

$$\frac{\partial p(X_t = x)}{\partial t} = \frac{1}{2}\frac{\partial^2 \sigma(x)^2 p(X_t = x)}{\partial^2 x} - \frac{\partial \mu(x) p(X_t = x)}{\partial x}. \tag{A3}$$

Its solution is the time-dependent distributions of X_t and it depends on the initial condition.

Acknowledgements

This work was supported by the DGA, Delegate for Armament of French MoD.

References

[1] K. Ward, C. Baker, and S. Watts, "Maritime surveillance radar. I. radar scattering from the ocean surface," *IEE Proceedings F - Radar and Signal Processing*, 1990.
[2] A. Farina, G. Gini, M. Greco, and L. Verrazzani, "High resolution sea clutter data: statistical analysis of recorded live data," *IEE Proceedings - Radar, Sonar and Navigation*, 1997.
[3] T. R. Field, *Electromagnetic Scattering from Random Media*. Oxford University Press, 2009.
[4] K. Ward, R. Tough, and S. Watts, *Sea Clutter: Scattering, the K distribution and Radar Performance*. 20, IET Radar, Sonar and Navigation, 2006.
[5] T. R. Field and S. Haykin, "Nonlinear dynamics of sea clutter," *International Journal of Navigation and Observation*, 2008. Special Issue on Modelling and Processing of Radar Signals for Earth Observation.
[6] F. Gini and M. Greco, "Texture modeling and validation using recorderd high resolution sea clutter data," *Proceedings of the 2001 IEEE Radar Conference*, 2001.
[7] L. Gallardo, *Mouvement brownien et calcul d'Itô*. Editions Hermann, 2008.
[8] H. Risken, *The Fokker-Planck Equation: methods of solution and applications*. Springer, 1989.
[9] E. Jakeman, "On the statistics of K-distributed noise," *Journal of Physics A: Mathematical and General*, vol. 13, no. 1, pp. 31–48, 1980.
[10] R. Tough, "A Fokker-Planck description of K-distributed noise," *Journal of Physics A: Mathematical and General*, vol. 20, no. 3, pp. 551–567, 1987.
[11] E. Jakeman and R. J. A. Tough, "Non-gaussian models for the statistics of scattered waves," *Advances in Physics*, vol. 37, no. 5, pp. 471–529, 1988.
[12] B. Oksendal, *Stochastic Differential Equations: An Introduction with Applications, Fifth Edition*. Springer-Verlag, 2000.
[13] S. Iyanaga and Y. Kawasa, *Encyclopedic dictionary of mathematics*. MIT press, 1980.
[14] M. Abramowitz and I. Stegun, *Handbook of Mathematical Functions*. National Bureau of Standards Applied Mathematics Series, 1964.
[15] G. Arfken and H. Weber, *Mathematical Methods for Physicists*. Elsevier Academic Press, 2005.
[16] "*NIST Digital Library of Mathematical Functions*." http://dlmf.nist.gov/, Release

1.0.15 of 2017-06-01. F. W. J. Olver, A. B. Olde Daalhuis, D. W. Lozier, B. I. Schneider, R. F. Boisvert, C. W. Clark, B. R. Miller and B. V. Saunders, eds.

[17] R. Muirhead, *Aspects of Multivariate Statistical Theory*. Wiley Series in Probability and Mathematical Statistics, 2005.

[18] P. Fayard and T. Field, "Optimal inference of the scattering cross-section through the phase decoherence," *Waves in Random and Complex Media*, vol. 18, no. 4, pp. 571–584, 2008.

[19] D. J. Higham, "An algorithmic introduction to numerical simulation of stochastic differential equations," *Society for Industrial and Applied Mathematics*, vol. 43, no. 3, pp. 525–546, 2001.